JOURNAL OF AIRCRAFT
Vol. 44, No. 6, November–December 2007

Effects of Strake Planform Change on Vortex Flow of a Double-Delta Wing

Myong H. Sohn* and Hyoung S. Chung†
Korea Air Force Academy, Choongbook-Do 363-849, Republic of Korea

DOI: 10.2514/1.30261

This study examines the effects of a strake planform change on the vortex characteristics of double-delta wings through wing-surface pressure measurements and the off-surface flow visualization of the wing-leeward flow region. Three different shapes of strakes (65/90 deg sweep cropped-delta, 79 deg sweep single-delta, and 72/84 deg sweep cropped-delta) were tested. The double-delta wing configuration with the 79 deg sweep single-delta shape strake produced a more concentrated vortex system at upstream locations and showed advanced coiling and downward movement of the strake and wing vortices compared with the other two configurations. However the concentrated vortex system for the double-delta wing configuration with the 79 deg sweep single-delta shape strake tended to diffuse and break down much faster than the other two configurations as the flow proceeded downstream. The test results reveal that strake modification can greatly alter the vortex flow pattern around a double-delta wing.

Nomenclature

c = chord length at wing root (or centerline)
s = wing local semispan
α = angle of attack
β = sideslip angle

I. Introduction

MODERN fighter aircraft of enhanced maneuverability have commonly adopted a straked-delta or a double-delta wing configuration. At high angles of attack, a highly swept strake or front wing generates stable vortex pairs and produces additional source of lift; moreover the strong strake vortex strengthens and stabilizes the main wing vortex, which results in improved lift-to-drag ratio performance and delay of vortex breakdown. Even though the strake-wing vortex interaction of a double-delta wing generally increases lift performance and stability, it can also cause unusual and nonlinear aerodynamic behavior when the angle of attack and/or sideslip angle exceeds certain limits, which results in severe departure and buffet phenomenon [1–3]. The development, interaction, and breakdown of the vortex system of double-delta wings are very sensitive to wing geometry and flow conditions such as sweep angles for the strake and the main wing, sharpness of the leading edges, angle of attack, and sideslip angle.

Many investigations have been made to understand the flow physics of the complicated vortex flows of double or straked-delta wings, and in some cases to find a way to control them. Hebbar et al. [2] evaluated the effects of juncture fillets on the vortex core trajectory and the vortex burst location of a double-delta wing at high angles of attack and sideslip angles. They employed water-tunnel visualization data to verify the change of the vortex trajectory and delay of the vortex breakdown by adding juncture fillets. Ericsson [3] provided valuable physical insight into double-delta wing flow by relating measurements of its highly unusual rolling-moment characteristics to the plausible vortex flow pattern of a 76/40 deg double-delta wing undergoing pitch oscillation. He concluded that the lateral aerodynamics at high angles of attack was dominated by the interaction between strake and wing vortices and the associated vortex breakdown. Frink and Lamar [4] did a water-tunnel study of the vortex breakdown characteristics for a large number of analytically designed vortex strakes, and concluded that one of the prime considerations in the strake design was the maintenance of a well-organized vortex system over the main wing to as high an angle of attack as possible. Kern [5] numerically investigated the effects of geometry modification (i.e., adding fillets) at the junction of the leading-edge extension (LEX) and the wing of a cropped double-delta shape. He suggested that fillets enhanced the lift and lift-to-drag ratio and could be used as a method of controlling the trajectory, interaction, and breakdown of the vortex system. Klute et al. [6] examined the effects of a drooping apex flap for fixed and pitching delta wings of 75 deg sweep angle. They employed visualization, wing-surface pressure measurements along the two rays, and LDV measurements of the wing-leeward wake section. They suggested that apex flap could delay vortex breakdown by an angle of 8 deg beyond the steady-flow breakdown angle of attack, and that this apex flap effect was equally pronounced in dynamic pitching. The breakdown position was estimated by a local slight increase in streamwise pressure distribution.

Lowson and Riley [7] examined systemically the reasons for variation of the vortex breakdown positions of delta wings with the same sweep angle and angle of attack that exists in a large body of delta-wing data and found that the effects on the vortex breakdown positions due to variations in geometry (i.e., thickness, leading-edge chamfers, leading-edge radius, and especially apex shape due to these geometry parameters) far outweighed those due to support interference, wind-tunnel factor, methods of flow visualization, and changes in Reynolds number. They also postulated that the vorticity shed from the apex formed the center of the vortex cores; hence the apex shape affected the vortex strength and structure of delta wings. Myose et al. [8] studied the effect of delta-wing shape on the leading-edge vortex breakdown by performing visualization in a water tunnel. Four different shapes (i.e., diamond, cropped-delta, single-delta, and double-delta) were tested. They showed that the cropped-delta wing had the longest unburst leading-edge vortex and the double-delta wing had the earliest vortex breakdown. Zhan and Wang [9] studied the effects of Gurney flaps and apex flaps on the longitudinal aerodynamic performance of a delta wing with 70 deg sweep angle through force and moment measurements. They suggested that the simultaneous use of apex and Gurney flaps could greatly improve longitudinal aerodynamic performance, and that the apex flap contributed much to the gains. If it exists, the flow physics data associated with the improved aerodynamic performance by the

Presented as Paper 3498 at the AIAA 3rd Flow Control Conference, San Francisco, CA, 5–8 June 2006; received 4 February 2007; revision received 27 April 2007; accepted for publication 27 April 2007.

*Professor, Department of Aerospace Engineering; myongsohn@hanmail.net. Senior Member AIAA.
†Assistant Professor, Department of Aerospace Engineering.

use of apex and Gurney flaps would be valuable. Sohn et al. [10–12] investigated the vortical flow of a 65 deg-sweep sharp-edged delta wing with a cropped-delta shape strake of 65/90 deg sweep through wing-surface pressure measurements and off-surface flow visualization tests of the wing-leeward flow region and compared them with the results for a plain delta wing to identify the effects of strake on the vortex flow over a delta wing. Their results confirmed the stabilizing effect of strake, and specifically that the vortex system of the double-delta wing with strake was stronger, more stabilized, and more breakdown resistant to sideslip. Once the usefulness of strake installation on a delta wing was verified, a further investigation on the effects of strake shape change was needed.

In the present study, the effects of strake planform shape on the vortex formation, interaction, and breakdown characteristics of double-delta wing configurations were investigated by conducting pressure measurements on the wing upper surface and by off-surface flow visualization of the wing-leeward flow region. Three different shapes of strakes (65/90 deg sweep cropped-delta, 79 deg sweep single-delta, and 72/84 deg sweep cropped delta) were tested. Each strake was attached to a 65 deg sweep-delta wing to form a double-delta wing configuration. The cases of 0 and −5 deg sideslip angles were investigated at the angles of attack of 24, 28, and 32 deg. In the present experimental study, wing-surface pressure measurements and off-surface flow visualization were carried out simultaneously so that the aerodynamic load characteristics of the double-delta wing with different strake shapes could be described with the flow physics observed.

II. Experimental Model and Techniques

A. Experimental Model

The experimental model was a flat wing with sharp leading edges and a 65 deg sweep angle. The sharp leading edges were obtained by beveling the lower surface by 25 deg and leaving the upper surface flat. The trailing edge was also beveled in the same way. The model had a root chord of 600 mm without the strake and a trailing edge span of 475.4 mm. Three strake shapes tested were 65/90 deg sweep cropped-delta (shape A), 79 deg sweep single-delta (shape B), and 72/84 deg sweep cropped-delta (shape C). Shape A represented a general cropped-delta wing configuration and shape B represented a general double-delta wing configuration, whereas shape C was the intermediate configuration between shapes A and B. The objective of this study was to investigate the effect of strake shape change only. Thus the main delta-wing configuration was fixed and the strakes were attached at the same location.

All strakes were flat plates of 6.35 mm thickness and had the same root chord of 330.2 mm. The leading and side edges of the strakes were symmetrically beveled. The apex portion of the delta wing could be removed and replaced with the strakes to form double-delta wing configurations with a root chord of 795 mm. Figures 1a and 1b show the strake planform and the geometry of the integrated configuration. The lower wing-surface was mounted with a fuselagelike structure that served as the housing for the pressure tubes and model support. Figure 1c shows a picture of the model installed in the wind tunnel.

The main wing was equipped with four spanwise rows of upper-surface static pressure taps for pressure measurements. The pressure rows were located at the 30, 43, 60, and 80% wing chord c) stations, measured from the main wing apex. There were 47 pressure taps on each chord station along the entire span, each one located at the same relative span position normalized by a local semispan s. The nearest pressure tap to the wing's leading edge was located at the $0.025s$ point from the sharp leading edge.

The off-surface visualization was done with a $\frac{2}{3}$ scale model, which had the same geometry as the model used in the wing-surface pressure measurement. The main wing of the visualization model had a root chord of 400 mm, a trailing edge span of 317 mm, and a thickness of 10 mm. The main wing was made with a Bakelite plate,

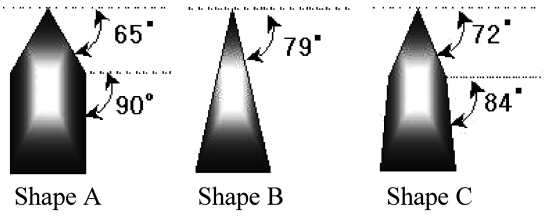

a) Strake planforms

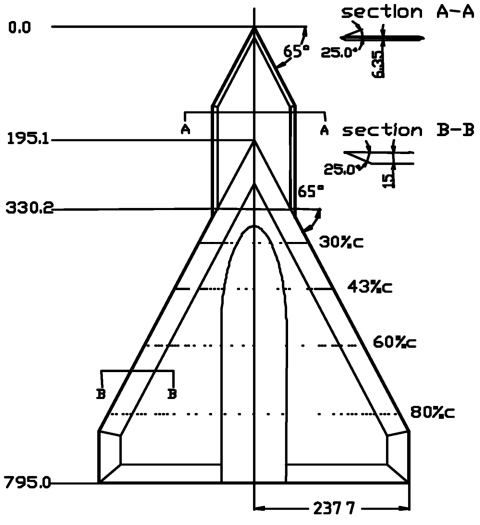

b) Geometry of complete model (Shape A)

c) Model in the test section

Fig. 1 Experimental models.

the strake of which was an aluminum plate of 4 mm thickness. The x direction was defined as the coordinate along the wing centerline measured from the wing apex, y as the coordinate along the wing local semispan measured from the wing centerline to the starboard-side wing, and z as the coordinate normal to the upper wing surface.

B. Experimental Technique

The wing-surface pressure measurement was performed at the Korea Air Force Academy Low-Speed Wind Tunnel. This medium-scale test facility is a closed-circuit atmospheric tunnel with a test section of 3.5 m(W) × 2.45 m(H) × 8.7 m(L) which can produce a maximum freestream velocity of 92 m/s. The contraction ratio is 7.26:1, flow angularity is less than 0.1 deg, and the axial turbulence intensity (u'/U) is 0.04% at the freestream velocity of 74 m/s.

Static pressure on the upper wing surface was measured by a PSI 8400 pressure measuring system. The measurement rate was 0.2 s/measure. The wing-surface pressure data in this study was an ensemble average of 300 pressure signals from each pressure tap. The freestream velocity was 40 m/s, which corresponds to the Reynolds number of 1.64×10^6. The angles of attack (α) tested were 24, 28, and 32 deg, and the sideslip angles (β) were 0 and −5 deg. An uncertainty analysis for pressure measurements was carried out following the procedures suggested in the AIAA Standard [13] to assess data accuracy and confidence level. It was estimated that the pressure measurement uncertainty in the present study was less than 24.86 Pa at 95% confidence level, which was about 0.36% F.S.

A method of using micro water droplets and laser beam sheet was developed for off-surface flow visualization. Water droplets of 5 ∼ 10 μm were generated by a home-style ultrasonic humidifier and a 3 W argon ion laser was used to generate the light sheet. The laser light sheet was perpendicular to the wing surface and the wing centerline. The illuminated planes were recorded by a high-resolution SONY DCR-VX 2000 NTSC digital camera. Details of the off-surface flow visualization employed in the present study are described in [11]. The off-surface visualization was made in another KAFA small-sized, low-speed wind tunnel with a test section size of 0.9 m(W) × 0.9 m(H) × 2.1 m(L). The freestream velocity of the off-surface visualization was 8 m/s, which corresponds to the Reynolds number of 2.2×10^5.

III. Results and Discussion

A. Zero Yaw Case

Figure 2 compares the wing-surface pressure distributions of the double-delta wings with strake A (shape A) and strake B (shape B) at $\alpha = 24$, 28, and 32 deg for the zero sideslip condition. The results show that at all angles of attack tested, shape B produces a much larger magnitude of suction pressure peaks than shape A at the two upstream chord stations (Figs. 2a and 2b). Also the suction pressure peaks of shape B are located more inboard than those of shape A. At the 30% chord station, the suction pressure peaks of shape A are located near the leading edge ($y/s \approx 1.0$), whereas those of shape B are located at about $y/s \approx 0.62$. It was found that the suction pressure peaks of shape A were generated by the wing vortices located adjacent to the wing leading edge, and that those of shape B were generated by the well-developed strake vortices located close to the wing surface. At the 43% chord station, the suction pressure peaks are rounded for shape A, whereas shape B maintains sharp pressure peaks. As the visualization results will later show, the different rate of coiling and consequential core movement of the strake and wing vortices traveling downstream made different pressure distribution characteristics for the two shapes. At the two downstream chord stations, the shape B suction pressure peaks reduced in magnitude significantly, as shown in Figs. 2c and 2d, and are also located more outboard than those of shape A at the 60 and 80% chord stations.

As indicated in Fig. 2, an excellent symmetry of the pressure distribution is observed at all angles of attack for shape A, but the symmetry of the pressure distribution is not guaranteed at $\alpha = 32$ deg for shape B. The dynamic images of visualization show that the vortex cores of shape B meandered considerably in both spanwise and chordwise directions at $\alpha = 32$ deg, whereas those of shape A did so a little. The asymmetry of the pressure distribution at $\alpha = 32$ deg for shape B is considered to be an intrinsic flow characteristic at high angles of attack. Myose et al. [8] conducted a visualization study on the effect of delta-wing shape on leading-edge vortex breakdown. They showed that the cropped-delta wing had the longest unburst leading-edge vortex and that the double-delta wing had the earliest vortex breakdown among the diamond, cropped-delta, single-delta, and double-delta shapes. In the present study, the results from the simultaneous off-surface flow visualization and the

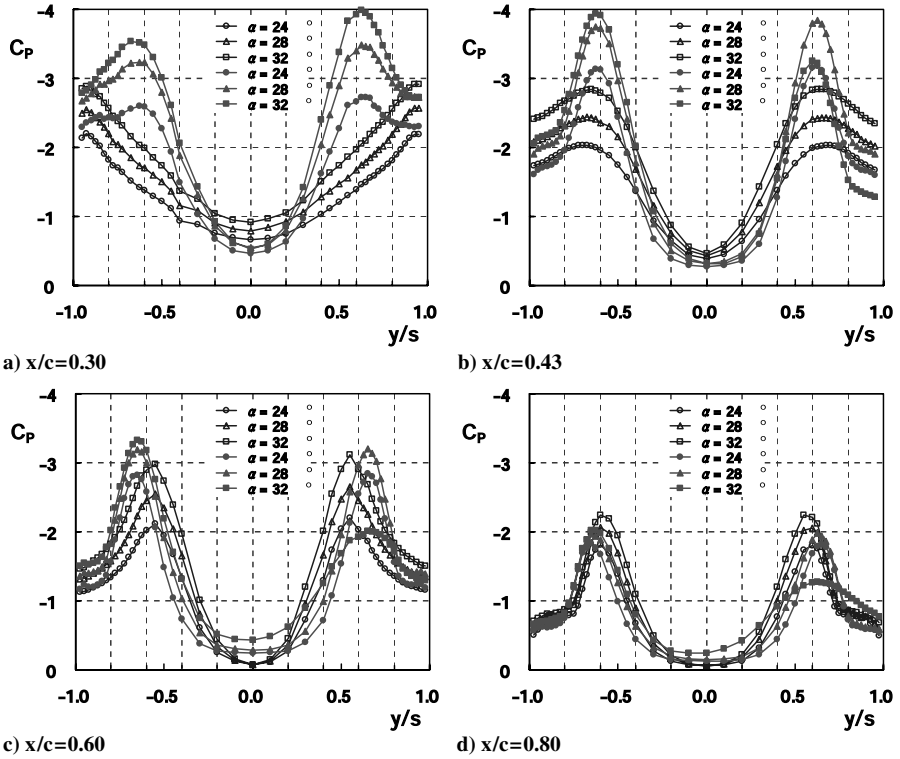

Fig. 2 Comparison of wing-upper-surface pressure distributions of shape A (blank symbols) and shape B (solid symbols) at $\beta = 0$ deg.

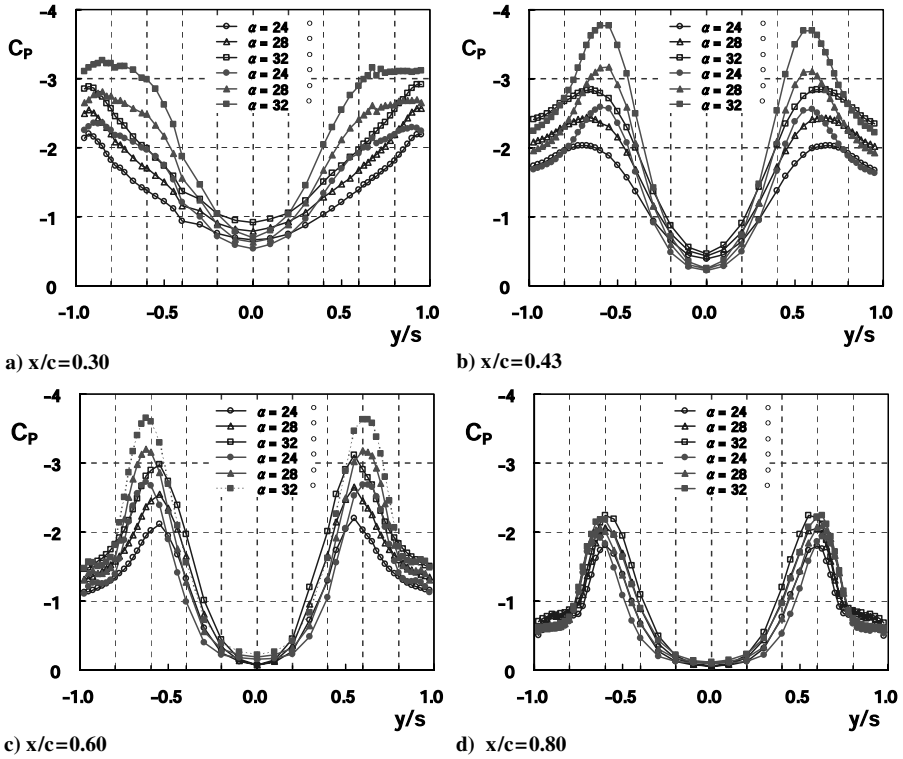

Fig. 3 Comparison of wing-upper-surface pressure distributions of shape A (blank symbols) and shape C (solid symbols) at $\beta = 0$ deg.

wing-surface pressure measurements also show that the vortex system for the double-delta wing with strake B (single-delta shape) is less stable than that of the double-delta wing with strake A (cropped-delta shape), as in Myose's results.

Figure 3 shows that the pressure distributions for shape C exhibit an intermediate trend between shapes A and B. At the two upstream chord stations, shape C has a smaller magnitude of suction pressure peaks than shape B, but a larger magnitude of suction pressure peaks than shape A. However the suction pressure peaks of shape C did not diminish significantly when going downstream as did those of shape B as shown in Fig. 3c. Also shape C maintained a fairly good symmetric pressure distribution up to the 80% chord station even at $\alpha = 32$ deg. The magnitude of the suction pressure peaks of shape C surpassed that of shape A at all angles of attack tested and at all chord stations except the 80% chord station. This observation supports Lowson and Riley's [7] conclusion that the apex geometry was the most important parameter affecting the delta-wing vortex flow. The intermediate pressure distribution characteristics of shape C, which is the intermediate shape between shapes A and B, as shown in Figs. 2 and 3, introduce the possibility of applying the strake planform modification for altering the vortex flow pattern around a double-delta wing.

Figure 4 compares the visualization results of shapes A and B at $\alpha = 24$ deg and $\beta = 0$ deg. At the 30% chord station (Figs. 4a and 4b), both shapes have well-developed strake vortices located inboard, and small but concentrated wing vortices adjacent to the wing leading edge. The strake vortices of shape B were located more inboard and closer to the wing-upper surface, which caused larger and more inboard-located suction pressure peaks for shape B, as shown in Fig. 2a. The strake and wing vortices on the left-half-wing rotated in a clockwise direction and the strake and wing vortices on the right-half-wing rotated in a counterclockwise direction. Two distinct vortex pairs of strake and wing vortices coiled and merged as they traveled downstream.

At the 43% chord station (Figs. 4c and 4d), the two distinct cores of the strake and wing vortices positioned themselves parallel to the upper-wing surface for shape A, whereas those for shape B positioned themselves vertically to the upper-wing surface. These relative positions of the strake and wing vortices for shapes A and B agree with the rounded suction pressure peaks for shape A and the sharp suction peaks for shape B, as shown in Fig. 2b. It is observed that the relative position of the strake and wing vortex cores for shape B at the 43% chord station (Fig. 4d) displayed a similar pattern to that for shape A at the 60% chord station (Fig. 4e), and the relative position of the strake and wing vortex cores for shape B at the 60% chord station (Fig. 4f) displayed a similar pattern to that for shape A at the 80% chord station (Fig. 4g). This indicates that the coiling and merging process of the strake and wing vortices was accelerated for shape B.

Olsen and Nelson [14] remarked that the first interaction point of the stake and wing vortices for the double-delta wing with strake moved upstream as the juncture angle (i.e., the angle difference

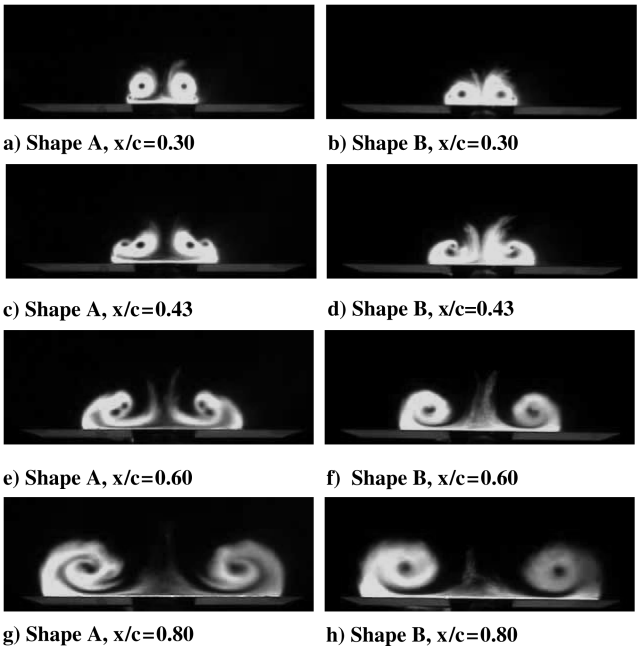

Fig. 4 Visualization result comparison of shapes A and B ($\alpha = 24$ deg, $\beta = 0$ deg).

between the strake sweep angle and the wing sweep angle) decreased. The same trend was also observed in Verhaagen et al.'s study [15], in which the juncture angle was termed as kink angle. The advanced interaction between the strake vortex and the wing vortex for shape B in the present study agrees with Olsen and Nelson's conclusion because the juncture angle for shape A was 25 deg and that for shape B was 14 deg.

Two adjacent vortices of the same rotating sense and unequal strength revolve around a center that lies on the connecting line of the two vortex cores and at the point of zero induced velocity such that the revolving center is closer to the core of the stronger vortex. Also two vortices of the same rotating sense spiral around each other while maintaining the identity of each vortex until they merge into a single vortex when the strengths of the two vortices are about the same. However lopsided coiling occurs as the strengths of the two vortices become uneven, as shown in [10,16]. The strake vortex of the present double-delta wing configuration became weaker as it moved downstream because vorticity feeding discontinued after the juncture between the strake and the main wing. However the strength of the wing vortex did not diminish as it moved downstream because vorticity was being continuously fed into it through the shear layer that connected the wing vortex core and the wing leading edge. Therefore we can assume that the coiling between the strake and wing vortices was dominated by the strake vortex at the upstream chord stations, whereas it was dominated by the wing vortex at the downstream chord stations, as shown in the visualization results of Fig. 4. This phenomenon can also explain the results of inboard shifting at the upstream chord stations and outboard shifting at downstream chord stations for the suction peaks of shape B, as identified in Fig. 2. Verhaagen et al. [15,17] had conducted wing-surface pressure measurements and visualization tests for the vortex flow about a 76/40 deg double-delta wing. They also found that the strake and wing vortices started to coil around each other at 10 deg angle of attack and beyond, and that the strake vortex moved closer to the wing-surface and more outboard, whereas the wing vortex moved upwards and inboard as a consequence of the coiling process. Their experimental results confirm the trends found in the present paper.

Shape B had a stronger strake vortex, which dominated the coiling process at the upstream chord stations inducing the pressure peaks to shift toward the strake vortex. However the accelerated coiling process for shape B promoted the merger of the strake and wing vortices much faster at the downstream chord stations where the vorticity kept being fed into the vortex system through the wing leading edges, which led the merged vortex core to shift outboard at the downstream chord stations. The visualization results and the wing-surface pressure distributions in the present study support the conclusion in Ericsson's study [3] that the lateral aerodynamics at high angles of attack were dominated by the interaction between the strake and wing vortices.

B. Yawed Cases

Figure 5 compares the pressure distributions of the double-delta wings with strake A and strake B at $\alpha = 24$, 28, and 32 deg for the nonzero sideslip case. The sideslip angle was -5 deg, such that the port side was the windward side, and starboard side was the leeward side. It was observed that the sideslip induced the suction pressure peaks on the windward side to increase in magnitude and move inboard, and those on the leeward side to decrease in magnitude and move outboard for both shapes A and B. The effects of yaw on the wing-surface pressure distribution of the double-delta wings were in good agreement with previous studies concerning the effects of sideslip angle [1,10].

The effect of yaw was more pronounced for shape B than for shape A. The windward suction pressure of large magnitude at the upstream chord stations diminished and even collapsed at the downstream chord stations. The tendency of the windward suction pressure decrease or collapse at the downstream chord stations was more pronounced for shape B than for shape A. For example, the windward suction pressure at $\alpha = 28$ deg for shape A did not collapse even at the 80% chord station, but that for shape B had already collapsed at the 60% chord station, as shown in Figs. 5c and 5d. It was observed that the suction pressure peaks at these two downstream chord stations were severely diminished or collapsed at all angles of attack tested for shape B. This collapsed suction pressure on the windward side implies a vortex bursting phenomenon. The pressure distribution characteristics indicated that shape B generated a more concentrated vortex system at the upstream chord stations

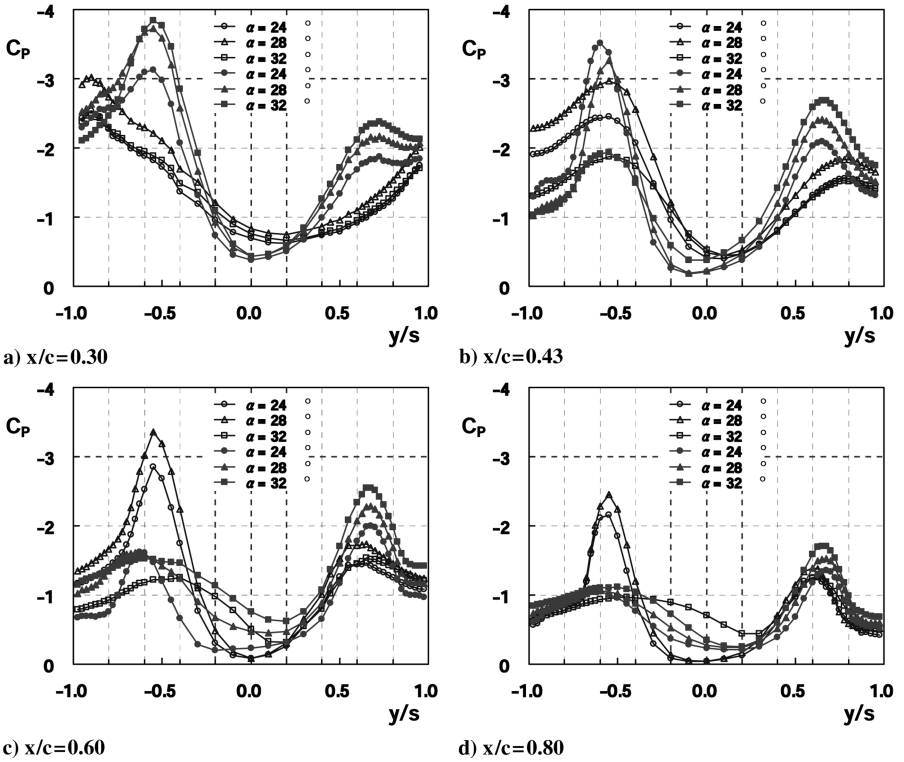

Fig. 5 Comparison of wing-upper-surface pressure distributions of shape A (blank symbols) and shape B (solid symbols) at $\beta = -5$ deg.

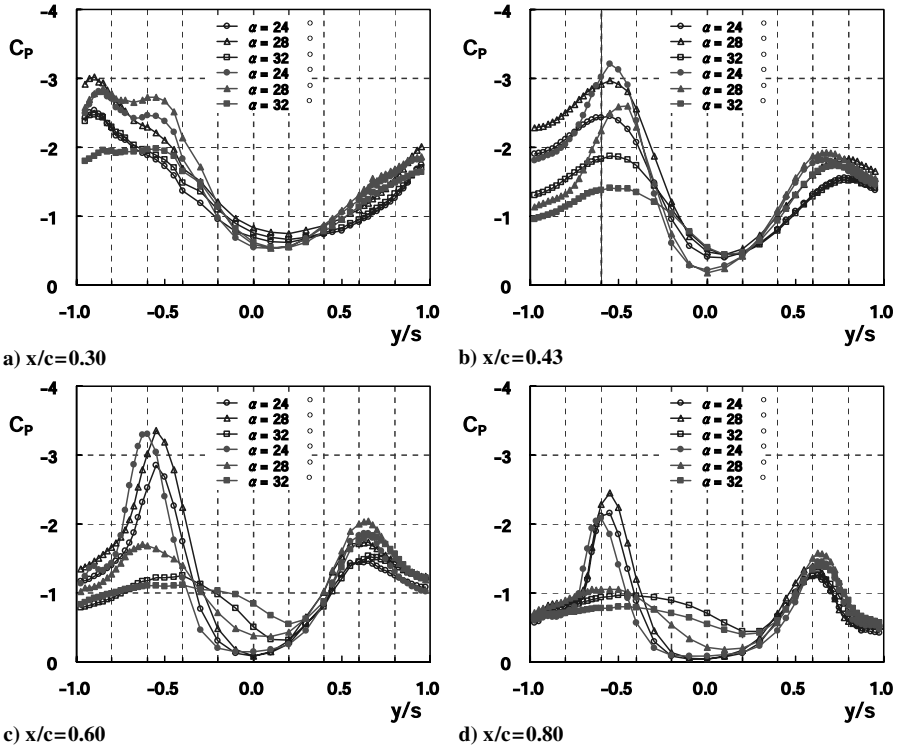

Fig. 6 Comparison of wing-upper-surface pressure distributions of shape A (blank symbols) and shape C (solid symbols) at $\beta = -5$ deg.

than did shape A, but that the vortex system of shape B was destabilized more rapidly and experienced a vortex burst as it moved downstream with increasing angles of attack. It was thus postulated that the accelerated interaction between the strake and wing vortices for shape B contributed to the breakdown of the vortices and earlier decay of the suction pressure for shape B.

Figure 6 compares the pressure distributions of the double-delta wings with strake A and strake C at $\alpha = 24$, 28, and 32 deg for $\beta = -5$ deg. Shape C had an intermediate suction pressure distribution between shapes A and B in terms of the magnitude of the suction pressure peak and the diminishing tendency of the suction pressure peaks at downstream chord stations and higher angles of attack. For example, at the 60% chord station the windward suction pressure of shape C exhibited a prominent peak at $\alpha = 24$ deg, exhibited a diminished peak at $\alpha = 28$ deg, and was completely collapsed at $\alpha = 32$ deg. At the same chord station, the windward suction pressure of shape B diminished at $\alpha = 24$ deg and collapsed at $\alpha = 28$ and 32 deg.

Figure 7 compares the visualization results for shapes A and B at $\alpha = 24$ deg and $\beta = -5$ deg, which shows that, compared with the zero sideslip case, the strake and wing vortices developed accelerated coiling and moved inboard and closer to the wing surface on the windward side, whereas they experienced delayed coiling and moved outboard and away from the wing surface on the leeward side. Comparing shapes A and B, the accelerated coiling of the strake and wing vortices and their closer movement to the wing surface were pronounced for shape B. In other words, the effect of sideslip was accentuated for shape B, which was a double-delta wing configuration with a highly swept delta-wing strake (79 deg sweep angle). However the accelerated merging process caused an earlier vortex burst on the windward side of shape B, as shown in Figs. 7f and 7h. These results support the collapsed suction pressure distribution on the windward side of shape B observed in Figs. 5c and 5d. Myose et al. [18] investigated the effect of a canard on delta-wing vortices by changing canard sweep angles. They found that, as the canard sweep angle increased, the vortex breakdown was accelerated and the vortex flow experienced full stall at lower angles of attack. The canards in Myose's work had the same effect on the vortex flow as the strakes did in the present paper.

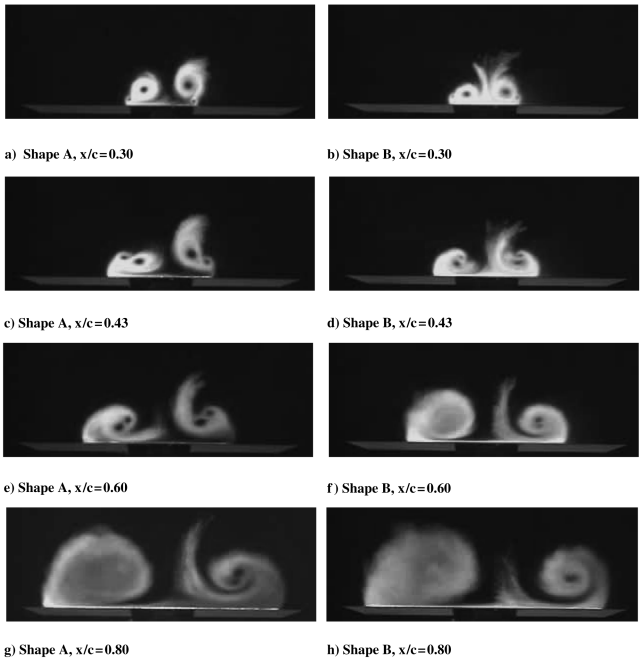

Fig. 7 Visualization result comparison of shapes A and B ($\alpha = 24$ deg, $\beta = -5$ deg).

The visualization results of Fig. 7 were overall in good agreement with the pressure distribution characteristics shown in Fig. 5 except for an earlier diffusion of the vortices in the visualization results. For example, the windward suction pressure distribution at the 80% chord station of shape A (Fig. 5d) had sharp peaks at both $\alpha = 24$ and 28 deg, which implies the existence of concentrated vortices of appreciable strength (i.e., no vortex burst), but the corresponding visualization result (Fig. 7g) shows the diffused vortices (i.e., vortex burst) on the windward side. The visualization was carried out at a Reynolds number of order-of-magnitude smaller (2.2×10^5) than the

pressure measurements (1.64×10^6) due to limitations of the visualization technique.

Even though it was reported by Hebbar et al. [19] and by Gursul et al. [20] that vortex interactions on double-delta wings may be very sensitive to Reynolds number at low Reynolds number range (below $Re = 0.1$ M), Verhaagen et al. [15] and Erickson [21] suggested in their studies that the onset of vortex bursting was independent of Reynolds number at high Reynolds number range (above $Re = 0.25 \sim 2.0$ M). The visualization results and surface pressure distributions obtained in the present study were well matched to each other in general except a couple of angles of attack cases for shape A, which followed the suggestions made by Verhaagen and Erickson. Therefore it is conjectured that the discrepancy between the visualization results and pressure distribution measurements for shape A did not result from the Reynolds effect. Instead the discrepancy might have come from the facts that the pressure measurements and the flow visualization tests had been conducted in different experimental conditions using different models. The vortex flow in the visualization, which was performed at a small freestream velocity (8 m/s) and low flow Reynolds number, reacted very sensitively to changes in the experimental conditions such as model geometry, support interference, and freestream disturbance.

IV. Conclusions

In this paper, the effects of strake planform changes on the vortex flow characteristics, and the resulting wing-surface pressure distribution of double-delta wings were investigated through pressure measurements on the wing upper-surface and off-surface flow visualization tests of the wing-leeward flow region. Three different shapes of strakes (65/90 deg sweep cropped-delta, 79 deg sweep single-delta, and 72/84 deg sweep cropped-delta) were tested.

The pressure measurement results indicated that the 79 deg sweep single-delta shape strake produced a more concentrated vortex system at upstream locations than the 65/90 deg sweep cropped-delta shape strake and the 72/84 deg sweep cropped-delta shape strake. However the concentrated vortex system for the double-delta wing configuration with the 79 deg sweep single-delta shape strake tended to diffuse and broke down much faster than that with the 65/90 deg sweep cropped-delta shape strake and the 72/84 deg sweep cropped-delta shape strake as the flow proceeded in a downstream direction. The off-surface flow visualization results also confirmed this trend identified from the wing-surface pressure measurement. The double-delta wing configuration with the 79 deg sweep single-delta shape strake showed advanced coiling of the strake and wing vortices and their downward movement compared with the other two configurations. Also the vortex system of the double-delta wing configuration with the 79 deg sweep single-delta shape strake diffused and broke down faster in the downstream region, causing flow instability.

The present study shows that the flow pattern around a double-delta wing can be greatly altered by modifications to the strake planform shape. The strake of intermediate shape resulted in intermediate vortex development and interaction characteristics as well as wing-surface pressure distribution characteristics. This introduces the possibility that the strake planform change can be used to alter the vortex flow around a delta wing.

Acknowledgment

This work was supported by the Basic Research Program of the Korea Science and Engineering Foundation (Grant Number R01-2003-10744-0).

References

[1] Grismer, D. S., and Nelson, R. C., "Double-Delta-Wing Aerodynamics for Pitching Motions With and Without Sideslip," *Journal of Aircraft*, Vol. 32, No. 6, 1995, pp. 1303–1311.

[2] Hebbar, S. K., Platzer, M. F., and Chang, W., "Control of High-Incidence Vortical Flow on Double-Delta Wings Undergoing Sideslip," *Journal of Aircraft*, Vol. 34, No. 4, 1997, pp. 506–513.

[3] Ericsson, L. E., "Vortex Characteristics of Pitching Double-Delta Wings," *Journal of Aircraft*, Vol. 36, No. 2, 1999, pp. 349–356.

[4] Frink, N. T., and Lamar, J. E., "Analysis of Strake Vortex Breakdown Characteristics in Relation to Design Features," *Journal of Aircraft*, Vol. 18, No. 4, 1981, pp. 252–258.

[5] Kern, S. B., "Vortex Flow Control Using Fillets on a Double-Delta Wing," *Journal of Aircraft*, Vol. 33, No. 6, 1993, pp. 818–825.

[6] Klute, S. M., Rediniotis, O. K., and Telionis, D. P., "Flow Control over a Maneuvering Delta Wing at High Angles of Attack," *AIAA Journal*, Vol. 34, No. 4, 1996, pp. 662–668.

[7] Lowson, M. V., and Riley, A. J., "Vortex Breakdown Control by Delta Wing Geometry," *Journal of Aircraft*, Vol. 32, No. 4, 1995, pp. 832–838.

[8] Myose, R. Y., Lee, B., Hayashibara, S., and Miller, L. S., "Diamond, Cropped, Delta and Double-Delta Wing Vortex Breakdown During Dynamic Pitching," *AIAA Journal*, Vol. 35, No. 3, 1997, pp. 567–569.

[9] Zhan, J., and Wang, J., "Experimental Study on Gurney and Apex Flap on a Delta Wing," *Journal of Aircraft*, Vol. 41, No. 6, 2004, pp. 1379–1383.

[10] Sohn, M. H., and Lee, K. Y., "Effects of Sideslip on the High-Incidence Vortical Flow of a Delta Wing with the Leading Edge Extension," AIAA Paper 2003-1107, 2003.

[11] Sohn, M. H., Lee, K. Y., and Chang, J. W., "Vortex Flow Visualization of a Yawed Delta Wing with Leading-Edge Extension," *Journal of Aircraft*, Vol. 41, No. 2, 2004, pp. 231–237.

[12] Sohn, M. H., and Lee, K. Y., "Experimental Investigation of a Yawed Delta Wing Having Leading Edge Extension," AIAA Paper 2002-3267, 2002.

[13] Anon, "Assessment of Experimental Uncertainty with Application to Wind Tunnel Testing," AIAA Standards Series, AIAA Paper S-071A, 1999.

[14] Olsen, P. E., and Nelson, R. C., "Vortex Interaction over Double Delta Wings at High Angles of Attack," AIAA Paper 1989-2191, 1989.

[15] Verhaagen, N. G., Jenkins, L. N., Kern, S. B., and Washburn, A. E., "Study of the Vortex Flow over a 76/40 deg Double-Delta Wing," AIAA Paper 1995-0650, 1995.

[16] Yu, F., Young, K., and Chang, R., "An Investigation on the Coiled-Up of Vortices on a Double Delta Wing," AIAA Paper 90-0382, 1990.

[17] Verhaagen, N. G., "Effects of Reynolds Number on Flow over 76/40-Degree Double-Delta Wings," *Journal of Aircraft*, Vol. 39, No. 6, 2002, pp. 1045–1052.

[18] Myose, R. Y., Hayashibara, S., Yeong, P. C., and Miller, S., "Effects of Canards on Delta Wing Vortex Breakdown During Dynamic Pitching," *Journal of Aircraft*, Vol. 34, No. 2, 1997, pp. 168–173.

[19] Hebbar, S. K., Platzer, M. F., and Fritzelas, A. E., "Reynolds Number Effects on the Vortical-Flow Structure Generated by a Double-Delta Wing," *Experiments in Fluids*, Vol. 28, No. 3, 2000, pp. 206–216.

[20] Gursul, I., Taylor, G., and Wooding, C. L., "Vortex Flows over Fixed-Wing Micro Air Vehicles," AIAA Paper 2002-0698, 2002.

[21] Erickson, G. E., "Water Tunnel Studies of Leading-Edge Vortices," *Journal of Aircraft*, Vol. 19, No. 6, 1982, pp. 442–448.